Observation of dynamic flux-line relaxation in ion-irradiated $Bi_2Sr_{1.8}CaCu_2O_x$ by Lorentz microscopy

K. Harada, H. Kasai, O. Kamimura, T. Matsuda, and A. Tonomura
Advanced Research Laboratory, Hitachi, Ltd., Hatoyama, Saitama 350-03, Japan

S. Okayasu and Y. Kazumata
Japan Atomic Energy Research Institute, Tokai, Naka-gun, Ibaraki 319-11, Japan
(Received 20 October 1995)

The dynamical behavior of individual flux lines in $Bi_2Sr_{1.8}CaCu_2O_x$ thin film irradiated with 240-MeV Au^{14+} ions was investigated by Lorentz microscopy. To evaluate the pinning effect of columnar defects, the irradiation to a single crystal was partially blocked by using a mask. The flux-line relaxation after changing the equilibrium conditions in the two regions, one irradiated and the other without irradiation, was observed simultaneously. Just after switching off the magnetic field at 4.5 K, the flux-line density in both regions decayed logarithmically with time from uniform configuration. However, the relaxation rate in the irradiated region was less than that in the nonirradiated region. The flux-line density in the equilibrium state in the irradiated region was much higher than that in the nonirradiated region. These results revealed that the pinning force was enhanced by ion irradiation. Also it was observed that reversely polarized flux lines are generated and pair annihilation occurs between opposite flux lines during the relaxation, which has never been revealed by conventional macroscopic techniques.

INTRODUCTION

The enhancement of the critical current density J_c of high-T_c superconductors is very important in practical applications. Obtaining large J_c requires strong pinning of flux lines because, when flux lines begin to move due to the Lorentz force induced by an electric current, a voltage is generated and this breaks down the superconducting state. To investigate the pinning mechanism and to identify the effective pinning centers, it is necessary to observe flux-line dynamics with pinning centers.

It has been reported that crystallographic defects and nonsuperconducting inclusions can improve J_c.[1] In particular, irradiation of high-T_c superconductors with electrons, neutrons, or ions is found to be effective in inducing these defects. In general, high energy electrons,[2,3] neutrons,[4] and light ions[5] create point defects and/or small defects whose pinning force is relatively small and they are effective only at low temperatures resulting in small increase in J_c. On the other hand, heavy ions with energy of hundreds of MeV (Refs. 6–9) create an amorphous region along their linear tracks[9] in the crystal of high-T_c superconductors. These columnar defects have been found to act as strong pinning centers of flux lines, especially for high-T_c superconductors with layered structure; thus they enhance the J_c.[10]

To investigate the interaction between columnar defects and flux lines, scanning tunneling microscopy (STM) for $NbSe_2$ (Ref. 11) and the Bitter technique for $Bi_2Sr_2CaCu_2O_x$ (Refs. 12 and 13) have been used for the static relation. However, flux-line dynamics cannot be observed by these techniques. On the other hand, with the Lorentz microscopy[14–16] and electron holography[17–19] which use a coherent electron beam, flux-line dynamics and the interaction with surface steps in Nb thin films can be observed.[16]

In the present work, the columnar defects produced by heavy ion irradiation on $Bi_2Sr_{1.8}CaCu_2O_x$ were investigated by observing the dynamic behavior of flux lines by Lorentz microscopy.

EXPERIMENTAL METHODS

A. Sample preparation

A single crystal of $Bi_2Sr_{1.8}CaCu_2O_x$ (BSCCO) with a size of $6\times6\times30$ mm^3 was prepared by standard floating zone methods using an imaging furnace. The critical temperature T_c of the crystal was about 87 K as determined by a superconducting quantum interference device (SQUID) magnetometer.

BSCCO films with thickness of 200–300 nm which were fairly uniform within a 100×100 μm^2 area were cleaved from the single crystal as specimens for transmission electron microscopy (TEM). The thin films were mounted on the low-temperature specimen stage of a 300-kV field emission electron microscope[20] similar to the one used in our previous works.[14–16,18,19]

B. Experimental setup

The experimental setup is illustrated in Fig. 1. The specimen was tilted to both the external magnetic field and the incident electron beam. The image of a single flux line is a spot consisting of bright and dark regions. The flux-line direction is along the line dividing the bright and dark regions, and the polarity is determined from the side on which the dark region is found.

The contrast of each single flux line depends on the angle at which the specimen is set to the horizontal and on the defocusing. The larger the setting angle of the specimen and the defocusing, the greater the contrast. In the present work, for the observation of a thicker specimen, the specimen was

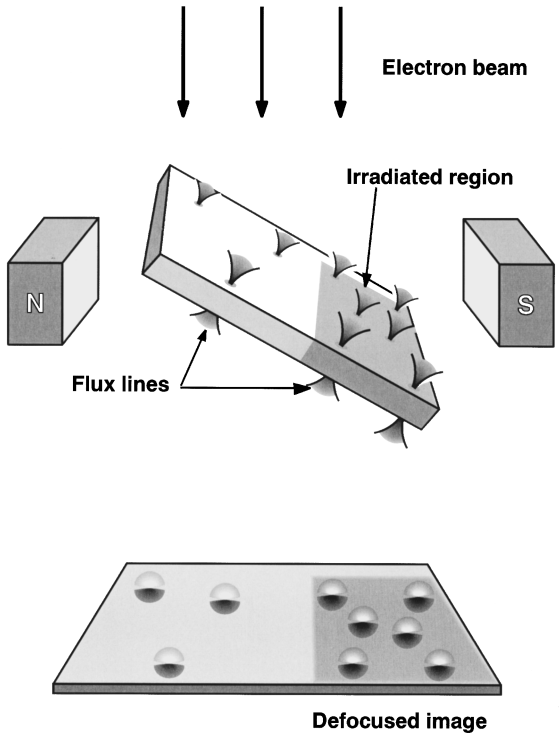

FIG. 1. Experimental arrangement of flux-line observation. The specimen is tilted 30° to the external magnetic field which is applied horizontally and 60° to the electron beam. Each flux line is observed as a spot consisting of bright and dark regions. The polarity is determined from the contrast.

mounted at 30° to the horizontal which was a smaller angle than that of previous experiments.[14–16] Therefore, a larger defocusing value, 112 mm, than used previously was needed to maintain the same contrast for observing the flux lines.

C. Ion irradiation

After cleaving the thin films for TEM observation, columnar defects were induced by 240-MeV Au^{14+} irradiation using a Tandem accelerator at the Japan Atomic Energy Research Institute (JAERI). To observe the effectiveness of pinning, both irradiated and nonirradiated regions were prepared in one specimen using a mask for the ion irradiation. A schematic diagram is shown in Fig. 2. Copper grids with a thickness of 50 μm and 25×25 μm^2 windows were used as the masks against ion irradiation. The irradiated and nonirradiated regions were observed simultaneously and the difference in dynamical behavior of the flux lines between the two regions was investigated by Lorentz microscopy.

The incident angle of Au^{14+} ions was a few degrees off the exact *c* axis because of slight bending and tilting of the thin films. Therefore, ion channeling, a phenomenon in which incident-charged particles are transmitted through the crystal without interaction, was automatically avoided and one ion produced a single columnar defect. The fluence measured by the electron counter corresponded to the density of columnar defects observed by TEM.

D. Magnetic properties

According to simulation,[21] the ion track of 240-MeV Au^{14+} in BSCCO consists of a 6-μm-long columnar defect

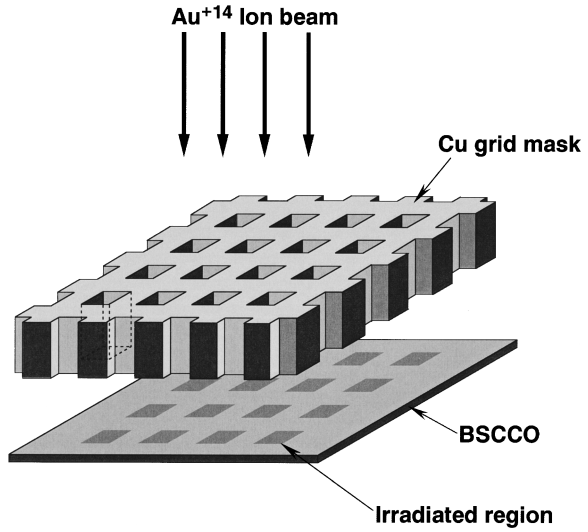

FIG. 2. Schematic diagram of ion irradiation. 240-MeV Au^{14+} ions are irradiated on cleaved BSCCO thin film through a 50-μm-thick Cu grid mask with 25×25 μm^2 windows. Both the irradiated and nonirradiated regions can be observed simultaneously by Lorentz microscopy.

and a 7-μm-long cascade. Therefore, to measure the effect of the columnar defects on the superconductor, the specimen thickness for the measurement had to be less than 6μm. One piece of 5-μm-thick BSCCO cleaved from the same single crystal was measured by the Quantum Design SQUID magnetometer before and after irradiation.

Figure 3 shows an example of the magnetization (*M*-*T*) curve before and after ion irradiation for a fluence of 3.1×10^8 ions/cm^2. The measurement was carried out as follows: (1) after cooling down the specimen with a magnetic field of 100 G, (2) the magnetic field was switched off, and (3) the specimen temperature was raised stepwise and magnetization was measured at each equilibrium temperature.

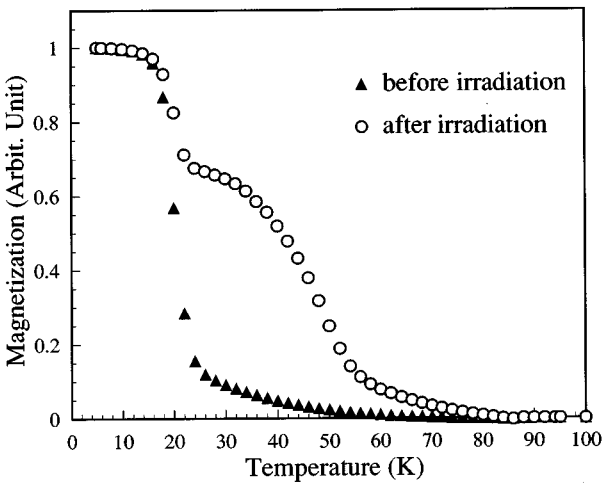

FIG. 3. The magnetization (*M*-*T*) curve of the BSCCO thin film at 100 G before (▲) and after (○) irradiation. After switching off the magnetic field, the magnetization is gradually decreased by raising the temperature. The shoulder above 22 K after irradiation shows the pinning effect enhanced by ion irradiation.

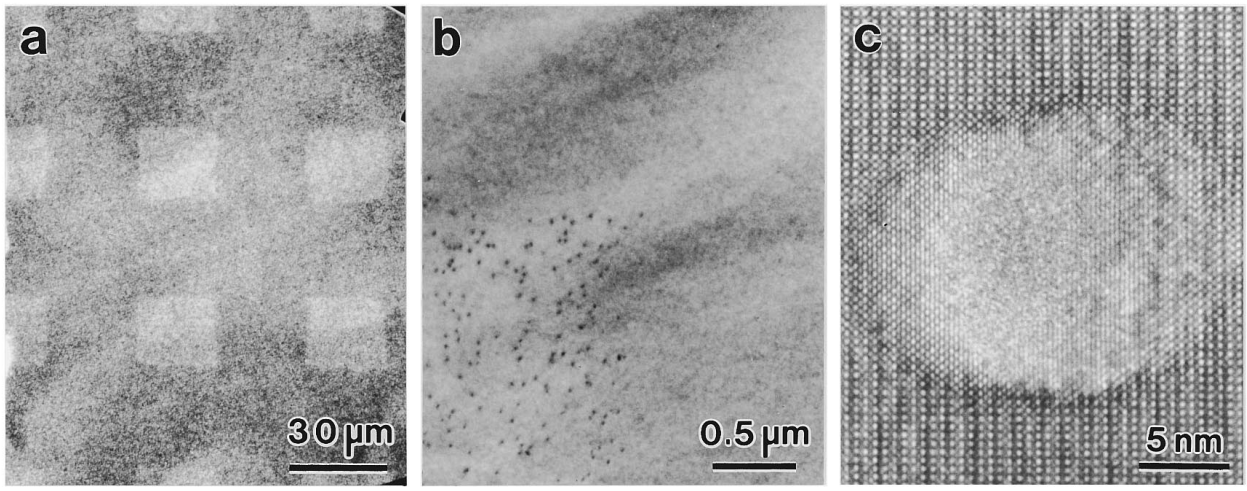

FIG. 4. Effect of 240-MeV Au^{14+} irradiation on a single crystalline BSCCO observed by electron microscopy: (a) scanning electron micrograph of a wide region, (b) transmission electron micrograph (bright field image) at one corner of an irradiated region, and (c) high-resolution electron micrograph of the columnar defect. Squares in (a) are irradiated regions and each black dot in (b) is a columnar defect induced by a single ion. The columnar defect is tilted a few degrees from the *c* axis in (c).

The shoulder in the magnetization curve above 22 K after irradiation shows that the pinning effect is enhanced by the columnar defects induced by ion irradiation. The effect of ion irradiation is seen by Lorentz microscopy, to observe the distribution and dynamical behavior of flux lines.

RESULTS AND DISCUSSION

A. The effect of ion irradiation

Figure 4 shows the results of heavy ion irradiation on BSCCO thin films. The scanning electron micrograph in Fig. 4(a) shows the distribution of the regions exposed under the mask windows by an irradiation of fluence of 10^{10} ions/cm^2. The transmission electron micrograph (bright field image) in Fig. 4(b) shows a magnified detail of a corner of the irradiated region. Each black dot in this figure corresponds to a single columnar defect induced by an ion. Columnar defects are found only in the unmasked regions so the Cu grid mask is effective in shielding against the ion beam. Figure 4(c) is a high-resolution micrograph recorded in the [001] direction of a columnar defect. The damaged area with an amorphous structure is about 10 nm in diameter and is spread out on either side of the micrograph, which suggests that the columnar defect was produced a few degrees off the exact *c* axis of the crystal.

B. Static configuration of flux lines

In the flux-line configuration shown in Fig. 5, the effect of ion irradiation was observed by making a comparison between the two regions. In Fig. 5(a), two irradiated regions can be seen as the parallelogram caused by tilting the specimen to the incident electron beam. This micrograph was recorded 5 min after switching off the external magnetic field of 10 G at 4.5 K. The flux lines in the irradiated regions are visible, but the contrast of flux lines outside these regions is lost because the flux lines in the nonirradiated region were flowing during the exposure time (40 sec). This shows that the flux-line configuration was not stable for 5 min after changing the condition. Since flux lines tend to flow along the boundary between the two regions, flux lines were not resolved at the boundary. These results are similar to those of our previous observation of Nb films.[16] Figure 5(b) is a magnified detail of one part of the parallelogram shown in Fig. 5(a) recorded 25 min after switching off the magnetic field. The arrows at the center of the micrograph point to a boundary between the irradiated region (left side) and the nonirradiated region (right side). The irradiated region includes many flux lines and some of these make a line along the boundary, whereas the nonirradiated region includes only a few flux lines in the same area. The unbalanced distribution and density of flux lines show the difference in average pinning force between the two regions caused by ion irradiation. Figure 5(c) is also an equilibrium configuration but with a larger magnetic field from a different experimental procedure. In the case of 5(c), the specimen was cooled to 4.5 K without a magnetic field, then a magnetic field of 40 G was applied and micrograph 5(c) was recorded 30 min later. The position of the boundary in the figure is similar to 5(b). The flux-line contrast was visible as vertical lines to the right side of the boundary (nonirradiated region), whereas the contrast to the left side (irradiated region) has disappeared. This is because the flux lines were randomly distributed by columnar-defect pinning in the irradiated region. Therefore, the contrast of the flux lines disappears because they overlap. On the other hand, in the nonirradiated region the flux lines make a regular lattice structure which can be seen as vertical lines.

Figure 5 shows that the flux-line configuration and the density strongly depend on ion irradiation. These results reveal the difference in average pinning force between irradiated and nonirradiated regions, i.e., the ion irradiation enhances the average pinning force of the material and the induced columnar defects suppress the flow of flux lines and disturb the regular lattice configuration.

C. Dynamical behavior of the flux-line relaxation

Lorentz microscopy showed the dynamical behavior of flux lines after the equilibrium conditions changed. One of

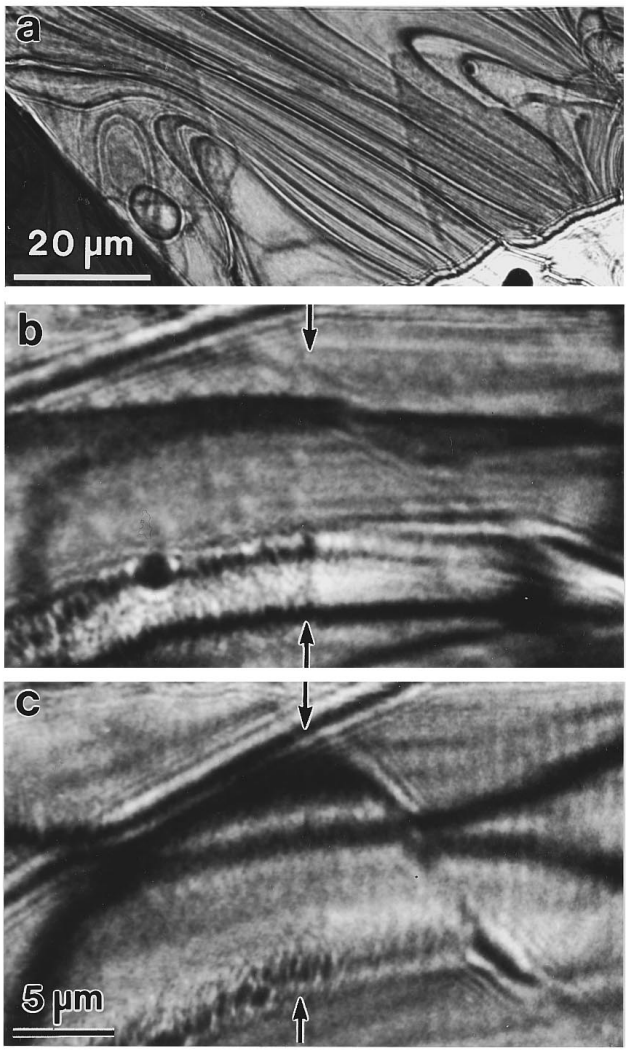

FIG. 5. Lorentz micrographs of BSCCO thin film including the irradiated regions: (a) flux-line configuration recorded 5 min after switching off the magnetic field of 10 G. Two irradiated regions (parallelogram) are visible by flux lines pinned in the columnar defects; (b) equilibrium configuration 25 min after switching off the magnetic field; (c) flux-line configuration after a magnetic field of 40 G was applied. The flux-line configurations and density in the micrographs are changed by the boundary between the irradiated (left side) and nonirradiated (right side) regions.

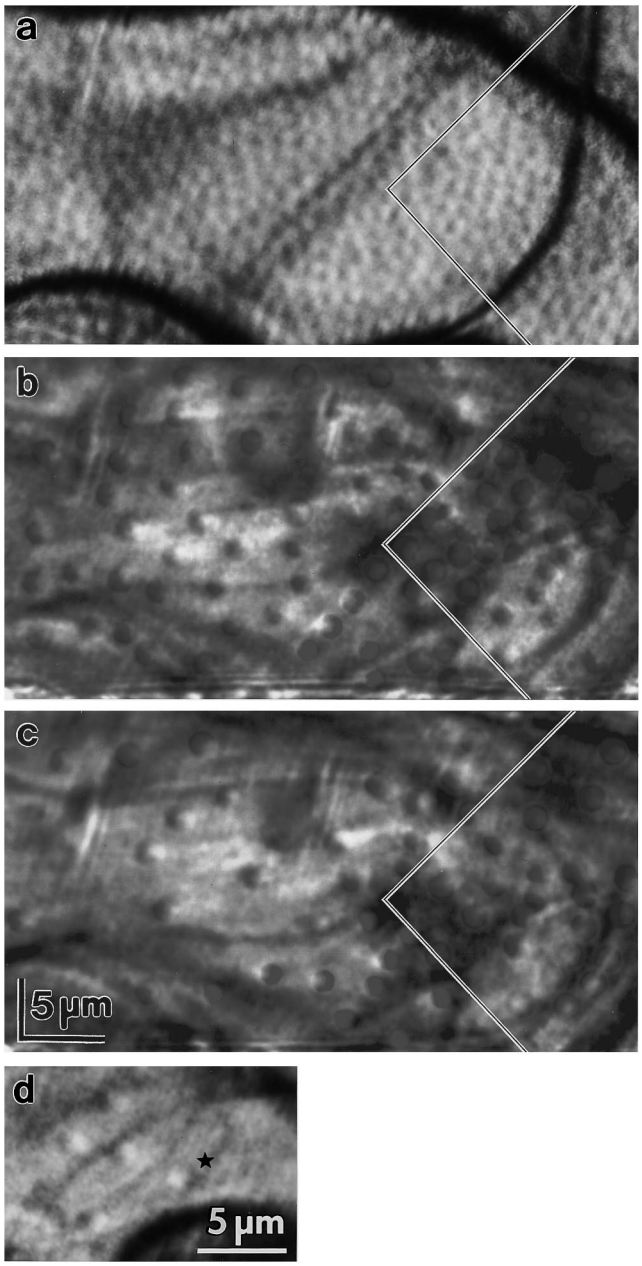

FIG. 6. Dynamic observation of flux-line decay when a magnetic field of 15 G is switched off: (a) within the magnetic field, (b) 26 min after switching off the magnetic field, (c) 58 min after switching off the field, and (d) the antiparallel flux lines observed in the relaxation process. The flux line indicated by ★ is a reversely polarized flux line. Initial flux lines (colored blue) in (b) and (c) decrease with time. Reversely polarized flux lines (colored red) are generated in the specimen and flow to the initial flux lines. The relaxation by pair annihilation probably occurs in this observation region.

these behaviors is a magnetic relaxation which is logarithmic decay of magnetization measured by a SQUID magnetometer. The relaxation process was thus directly observed in the unit of a single flux line.

Figure 6(a) shows a Lorentz micrograph of the area near the specimen edge, containing both irradiated and nonirradiated regions, which were cooled to 4.5 K with a magnetic field of 15 G. The boundary of the two regions is indicated on the figure. The density of flux lines corresponds to the external magnetic field. Although the density was uniform in the equilibrium condition [Fig. 6(a)] and just after switching off the magnetic field, the density in both regions gradually decayed with time. Figures 6(b) and 6(c) are relatively short exposure (5 sec) micrographs of the decay, which were recorded [6(b)] 26 min and [6(c)] 58 min, respectively, after switching off the magnetic field. To trace each flux line in the decay process easily and in high contrast, micrographs 6(b) and 6(c) were recorded with larger defocusing (152 mm) than 6(a); hence the flux lines colored blue and red appear to be larger than those in 6(a). The polarity of all of the flux

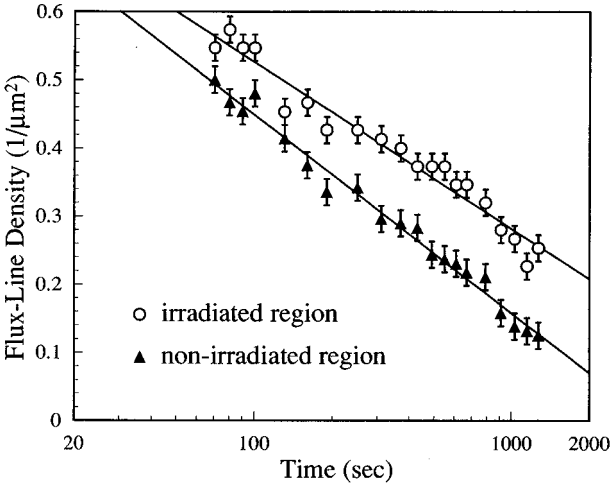

FIG. 7. Transition of flux-line density in both the irradiated (○) and nonirradiated (▲) regions. The density in both regions decays logarithmically with time. The relaxation rate (gradient) in the irradiated region is smaller than in the nonirradiated region. The difference in relaxation rates shows the pinning effect of the induced columnar defects.

lines in 6(b) and 6(c) is determined from their contrast, initial flux lines are colored blue and reversely polarized flux lines are colored red. The reason for observing both the flux lines at the same time is explained later. Figure 6(d) is an example of the antiparallel flux lines observed in this relaxation process. At the flux line indicated by a star, the bright and dark contrast in the flux line is reversed.

It is very difficult to record the relaxation process within 20 min of switching off the magnetic field, such as from Figs. 6(a)–6(b), since flux lines quickly flow out of the film one after another, for example, in Fig. 5(a). However, it is possible to record the relaxation on videotape. The motion of flux lines seemed not to ''hop'' between pinning centers as observed in Nb,[14,16] but to ''flow'' in the specimen. It is conjectured that the diameter of the flux lines (400 nm) was comparable to the hopping distance.

Also, a relaxation process was found by observing the dynamical behavior of flux lines in the series of Fig. 6. The flux-line density decays gradually with time in both regions and the difference in density between the two regions is extended. Twenty minutes after switching off the magnetic field, the initial flux lines (colored blue) decrease to less than 0.2 flux lines/μm^2. Then, the reversely polarized flux lines (colored red) begin to appear in the visual area [Fig. 6(b)] and increase in number with time [Fig. 6(c)]. The reversely polarized flux lines and this kind of relaxation have never been observed on nonirradiated or whole-area-irradiated specimens. Therefore, this relaxation process seems to depend on the distribution of remanent flux lines pinned by the columnar defects.

This process can be explained by a simple model. The flux lines pinned by the columnar defects, and their unbalanced distribution in the relaxation process, produced the reversely polarized flux lines at the edge of the superconducting thin film [Fig. 6(b)]. Then the flux lines increased in number with time [Fig. 6(c)] and were gradually attracted to the high-density region of the initial flux lines. There, they and the initial flux lines pinned at the columnar defects were annihilated when they met.

This generation of reversely polarized flux lines and the occurrence of pair annihilation cannot be observed by macroscopic techniques, which reveal them merely as the macroscopic relaxation. Our Lorentz microscopy, however, revealed the details of the relaxation process by showing the individual flux lines and their polarities dynamically.

Furthermore, to investigate the relatively rapid relaxation of the flux lines shown in Fig. 6, the dynamics of each flux line was traced and the densities in both regions were measured from successive frames (1/30 sec) of videotape. Figure 7 shows the density versus logarithm of time in both regions within 20 min after switching off the magnetic field [before recording Fig. 6(b)]. The density $D(t)$ in both regions decreases logarithmically with time. These logarithmic decays are similar to the results of the magnetization relaxation measured by a SQUID. The normalized relaxation rate $S=-1/D_0[dD/d(\ln t)]$ can be calculated using the data. The value of S is 0.13 for the nonirradiated region, and is 0.11 for the irradiated one. The decay rate in the nonirradiated region is about 20% larger than that of the irradiated region. This ratio is similar to the results from Cu^{11+} ion irradiation on BSCCO.[22]

CONCLUSION

Our Lorentz microscopy confirmed that columnar defects induced by heavy ion irradiation act as pinning centers in high-T_c BSCCO thin film, by comparing ion-irradiated and nonirradiated regions. The pinning effects were shown in the configuration and the dynamical behavior of flux lines after changing the equilibrium conditions. The logarithmic decay of the flux-line density is similar to that revealed by macroscopic observation. Furthermore, it was observed that the relaxation consists of two processes: the generation of reversely polarized flux lines and the pair annihilation of oppositely polarized flux lines.

ACKNOWLEDGMENTS

The BSCCO samples used in this work were provided by Dr. H. Tsuiki of Hitachi Chemical Co., Ltd. The authors are grateful to Dr. S. Ikeda of the National Research Institute for Metal and Professor H. Mori of the Research Center for Ultra-High Voltage Electron Microscopy of Osaka University for their valuable discussions about the effect of radiation on the materials. The authors are also grateful to Dr. F. Nagata and T. Shimotsu of Hitachi Instrument Engineering Co., Ltd. for their help in high resolution observation and for valuable discussions. Thanks are also due to Dr. M. Yamasaki, Dr. R. Sugano, Dr. T. Onogi, and Dr. N. Osakabe of Hitachi, Ltd. for their valuable advice and suggestions. We would like to thank S. Kubota, S. Matsunami, and N. Moriya of Hitachi, Ltd. for their technical assistance with the experiments.

[1] S. Jin *et al.*, Appl. Phys. Lett. **56**, 1287 (1990).
[2] M. A. Kirk, Cryogenics **33**, 235 (1993).
[3] S. Okayasu *et al.*, Physica B **194-196**, 1881 (1994).
[4] H. W. Weber, Supercond. Sci. Technol. **5**, S19 (1992).
[5] L. Civale *et al.*, Phys. Rev. Lett. **65**, 1164 (1990).
[6] W. Gerhäuser *et al.*, Phys. Rev. Lett. **68**, 879 (1992).
[7] Y. Zhu *et al.*, Phys. Rev. B **48**, 6436 (1993).
[8] H. Kumakura *et al.*, Jpn. J. Appl. Phys. **31**, L1408 (1992).
[9] B. Chenevier *et al.*, Jpn. J. Appl. Phys. **31**, L777 (1992).
[10] J. R. Thompson *et al.*, Appl. Phys. Lett. **60**, 2306 (1992).
[11] S. Behler *et al.*, Phys. Rev. Lett. **72**, 1750 (1994).
[12] M. Leghissa *et al.*, Phys. Rev. B **48**, 1341 (1993).
[13] H. Dai *et al.*, Science **265**, 1552 (1994).
[14] K. Harada *et al.*, Nature **360**, 51 (1992).
[15] K. Harada *et al.*, Phys. Rev. Lett. **71**, 3371 (1993).
[16] K. Harada *et al.*, Jpn. J. Appl. Phys. **33**, 2534 (1994).
[17] A. Tonomura, *Electron Holography* (Springer, Heidelberg, 1993).
[18] J. E. Bonevich *et al.*, Phys. Rev. Lett. **70**, 2952 (1993).
[19] J. E. Bonevich *et al.*, Phys. Rev. B **50**, 567 (1994).
[20] T. Kawasaki *et al.*, Jpn. J. Appl. Phys. **29**, L508 (1990).
[21] X. Gao *et al.*, Physica C **250**, 325 (1995).
[22] H. Kumakura *et al.*, J. Appl. Phys. **74**, 451 (1993).